

1           **A Novel Cell Therapy for COVID-19 and Potential Future Pandemics:**  
2                                   **Virus Induced Lymphocytes (VIL)**

3  
4   Rohan Sivapalan<sup>a</sup>, Jinyan Liu<sup>b</sup>, Krishnendu Chakraborty<sup>a</sup>, Elisa Arthofer<sup>a</sup>,  
5   Modassir Choudhry<sup>a</sup>, Philip S Barie<sup>d</sup>, Dan H Barouch<sup>§b,c</sup>, Tom Henley<sup>§a</sup>

6  
7   <sup>a</sup>Intima Bioscience, Inc. New York, NY, USA

8   <sup>b</sup>Center for Virology and Vaccine Research, Beth Israel Deaconess Medical Center, Harvard  
9   Medical School, Boston, MA, USA

10   <sup>c</sup>Ragon Institute of Massachusetts General Hospital, Massachusetts Institute of Technology,  
11   and Harvard University, Cambridge, MA, USA

12   <sup>d</sup>Division of Trauma, Burns, Acute and Critical Care, Department of Surgery; and Division of  
13   Medical Ethics, Department of Medicine, New York-Presbyterian Hospital/Weill Cornell  
14   Medical Center, Weill Cornell Medicine, New York, NY, USA

15  
16  
17  
18   <sup>§</sup>Co-corresponding Authors:

19   Tom Henley, [tom@intimabioscience.com](mailto:tom@intimabioscience.com);

20   Dan Barouch, [dbarouch@bidmc.harvard.edu](mailto:dbarouch@bidmc.harvard.edu)

21  
22  
23  
24  
25  
26  
27  
28  
29  
30  
31  
32  
33  
34  
35  
36

37 ABSTRACT

38

39 **Key words:** COVID-19; SARS-CoV-2; Adoptive Cell Therapy; T Cell Immunotherapy; Virology;  
40 Vaccinology; Immuno-virology; Allogeneic

41

42 The *a priori* T cell repertoire and immune response against SARS-CoV-2 viral antigens may explain the  
43 varying clinical course and prognosis of patients having a mild COVID-19 infection as opposed to those  
44 developing more fulminant multisystem organ failure and associated mortality. Using a novel SARS-  
45 Cov-2-specific artificial antigen presenting cell (aAPC), coupled with a rapid expansion protocol (REP)  
46 as practiced in tumor infiltrating lymphocytes (TIL) therapy, we generate an immune catalytic quantity  
47 of Virus Induced Lymphocytes (VIL). Using T cell receptor (TCR)-specific aAPCs carrying co-stimulatory  
48 molecules and major histocompatibility complex (MHC) class-I immunodominant SARS-CoV-2  
49 peptide-pentamer complexes, we expand virus-specific VIL derived from peripheral blood  
50 mononuclear cells (PBMC) of convalescent COVID-19 patients up to 1,000-fold. This is achieved in a  
51 clinically relevant 7-day vein-to-vein time-course as a potential adoptive cell therapy (ACT) for COVID-  
52 19. We also evaluate this approach for other viral pathogens using Cytomegalovirus (CMV)-specific  
53 VIL from donors as a control. Rapidly expanded VIL are enriched in virus antigen-specificity and show  
54 an activated, polyfunctional cytokine profile and T effector memory phenotype which may contribute  
55 to a robust immune response. Virus-specific T cells can also be delivered allogeneically via MHC-typing  
56 and patient human leukocyte antigen (HLA)-matching to provide pragmatic treatment in a large-scale  
57 therapeutic setting. These data suggest that VIL may represent a novel therapeutic option that  
58 warrants further clinical investigation in the armamentarium against COVID-19 and other possible  
59 future pandemics.

60

61

62

63

64

65

66

67

68

69 **MAIN**

70 Adoptive Cell Therapies (ACT) utilizing autologous patient-derived Tumor Infiltrating Lymphocytes  
71 (TIL) have demonstrated reproducible clinical responses in the setting of highly immunogenic tumors  
72 such as melanoma and HPV derived cervical cancer. With neoantigen enrichment, this demonstrable  
73 clinical efficacy has been extended to common epithelial solid tumors<sup>1, 2</sup>. The efficacy of TIL cell  
74 therapy relies on antigen specificity to the cognate cancer neoantigen, and on the ability to expand a  
75 large quantity of autologous or allogeneic cancer antigen-specific T cells *ex vivo*, and deliver this  
76 number back to the patient to enable cytolysis of the tumor cells and eradication of the cancer<sup>3, 4</sup>.  
77 Likewise, antigen-specific T cells are critical for an effective cellular immune response during infection  
78 with viral pathogens, and activation of cytotoxic T cells can clear an infection by killing virus-infected  
79 cells<sup>5, 6, 7, 8</sup>. Thus, we propose a similar-in-principle novel antigen-specific adoptive T cell therapy for  
80 viral infection predicated on precise T cell viral antigen-specificity. However, this viral platform  
81 requires cell kinetic expansion in days not weeks, thus allowing for the adoptive transfer of  
82 immunologically competent T cells in a therapeutically relevant time course in the setting of acute  
83 viral infection.

84 Like their tumor-resident counterparts, TIL, Virally-Induced Lymphocytes, or VIL, represent  
85 those T cells that have been activated in response to TCR-mediated, antigen-specific recognition of  
86 protein epitopes from viral particles<sup>9, 10</sup>. Cytotoxic CD8<sup>+</sup> T cells play a crucial role in mediating viral  
87 clearance in response to many respiratory viral infections including respiratory syncytial virus (RSV),  
88 influenza and coronavirus (CoV)<sup>5</sup>. Recent evidence has also demonstrated a critical role for the T cell  
89 immune response in the pathogenesis of the recently emerged COVID-19 disease, caused by the novel  
90 SARS-CoV-2 coronavirus<sup>11, 12, 13, 14</sup>. In addition to the readily detectible humoral immune response in  
91 the context of neutralizing antibodies in convalescent patients who had recovered from COVID-19,  
92 these studies have collectively shown strong SARS-CoV-2-specific memory T cells are frequently  
93 observed<sup>11, 13</sup>. Furthermore, significantly larger T cell responses appear to correlate with severity of  
94 the disease, underscoring the importance of T cells above and beyond the humoral antibody response  
95 for combating infection<sup>11</sup>. This is an important consideration for a novel therapeutic, as most  
96 prophylactic vaccines currently in development for COVID-19 are designed to focus on eliciting  
97 antibody responses to the spike protein of SARS-CoV-2<sup>15, 16, 17, 18, 19, 20, 21, 22, 23, 24</sup>.

98 In addition, the antibody response in recovered COVID-19 patients has been shown to decline  
99 several months after infection, raising concerns that therapeutics or vaccines designed to elicit  
100 primarily neutralizing antibody responses may not be sufficient to engender the cellular immunity  
101 required for long-term duration of protection or to protect from potential repeat infections<sup>25</sup>. Thus,  
102 the *a priori* T cell repertoire, both quantity and quality, may portend COVID-19 disease prognosis and

103 may influence the outcome between mild or severe disease. The treatment of patients with  
104 convalescent sera has recently been given US FDA Emergency Use Authorization (EUA)<sup>26</sup>. The transfer  
105 of neutralizing antibodies reflects a more *passive* serological immune engagement versus the more  
106 *active* cellular immune response that SARS-CoV-2-specific T cells would provide.

107 In an evolution of the cGMP methods for the expansion of TIL for the treatment of cancer that  
108 the researchers employ in a currently active human clinical trial<sup>27</sup>, we sought to develop an adoptive  
109 T cell therapy for COVID-19 based on rapid *ex vivo* expansion of SARS-CoV-2 antigen-specific VIL. Given  
110 the crucial importance of a strong virus-specific T cell response for patients with severe disease,  
111 especially during the critical days where respiratory distress is common, the adoptive transfer of a  
112 quantity of expanded, activated, effector memory T cells capable of mounting a robust virus-specific  
113 response may be important to reduce viral load and improve patient outcomes. Thus, we designed a  
114 T cell expansion platform comprising of microbead-based artificial antigen-presenting cells (aAPCs),  
115 we termed VIPR-particles (VIL-inducing particles R<sub>x</sub>), that carry MHC pentamer-peptide or tetramer-  
116 peptide complexes, specific for immunodominant SARS-CoV-2 epitopes, coupled with costimulatory  
117 anti-CD28 antibodies.

118 Using Peripheral Blood Mononuclear cells (PBMCs) isolated from convalescing COVID-19  
119 patients to represent what may be achievable in the clinic for patients actively suffering from the  
120 severe disease, we show that these TCR-specific aAPCs can expand virus-specific VIL up to 1,000-fold  
121 over a rapid and minimal culturing duration of just 7-days. Furthermore, these expanded VIL are  
122 enriched in virus antigen-specificity, show polyfunctional cytokine responses and acquire a T effector  
123 memory phenotype, making them highly suited for participating in an active cellular immune response  
124 when adoptively transferred back to patients after this minimal *ex vivo* expansion time. We also  
125 demonstrate the broad clinical potential of this platform and its modularity beyond COVID-19 and  
126 show in the setting of CMV infection that VIL specific for immunodominant CMV epitopes can also be  
127 expanded up to 1,000-fold using CMV-specific VIPR particles over a 7-day culture.

128 There are unfortunately limited therapeutic options for the treatment of COVID-19 that have  
129 demonstrated robust clinical relevance amidst the ongoing pandemic. Considerable,  
130 contemporaneous actual experience in the critical care of COVID-19 patients dating from the first  
131 quarter of 2020 in New York City, NY, USA, including observations of the clinical time course, hallmark  
132 clinical features, and treatment from presentation through critical illness to ultimate resolution or  
133 mortality, provides guidance as to the need for a vein-to-vein time of 7-days in order to intercede  
134 timely. A protective virus-specific T cell therapy may be an important novel modality for the treatment  
135 of SARS-CoV-2 and other pandemic viral pathogens.

136



137 **RESULTS**

138

139 *The detection and enrichment of antigen-specific Virus Induced Lymphocytes (VIL) in CMV*  
140 *infected individuals*

141

142 To develop a platform for robust and rapid *ex vivo* expansion of viral antigen-specific T cells from  
143 patients exposed to viral pathogens, we generated a micro-aAPC capable of providing an  
144 immunogenic viral peptide in the context of MHC Class I or MHC Class II molecules in combination  
145 with anti-CD28 stimulation molecules (Fig. 1a). MHC-I pentamers or MHC-II tetramers with associated  
146 viral antigen peptide complexes, along with anti-CD28 antibodies, were conjugated to 2.8  $\mu\text{m}$   
147 superparamagnetic beads with a monolayer of streptavidin covalently coupled to the surface. We  
148 termed these microbead-based aAPCs VIPR particles, and selected immunodominant viral antigens of  
149 known MHC specificity to demonstrate their capacity for TCR stimulation and simultaneous expansion  
150 of responding T cells. T cells isolated from donor PBMCs were cultured with these VIPR particles for 7-  
151 days in the presence of high concentrations of trophic cytokines, IL-2, IL-7 and IL-15 and addition of  
152 N-acetylcysteine (NAC), known to improve T cell proliferation<sup>28</sup>. As a validated control to demonstrate  
153 efficacy of the platform, we selected an immunodominant MHC-I restricted pp65 antigen of  
154 cytomegalovirus (CMV) known to robustly stimulate the TCRs of CMV-specific T cells<sup>29</sup>.

155 Individuals that have been previously exposed to CMV infection have recirculating virus-  
156 specific T cells (VIL) in their blood with TCRs specific for a variety of antigenic CMV peptides<sup>30</sup>. Using  
157 fluorescently conjugated pentamers and flow cytometry we analyzed the CD3<sup>+</sup> T cells isolated from  
158 the PBMCs of several independent CMV positive individuals and found approximately 0.2% of T cells  
159 were CD8<sup>+</sup> cells demonstrating specificity for the CMV pp65 antigen (Fig. 1b). After a 7-day culture  
160 with VIPR particles, these cells enriched on average 20-fold, reaching Pentamer<sup>+</sup>/CD8<sup>+</sup> T cell  
161 proportions of over 4% (Fig. 1b&c). By comparison, donor T cells cultured in cytokine alone in the  
162 absence of VIPR particles showed a minimal enrichment in antigen-specific VIL proportions, even  
163 though the T cells proliferated robustly. In addition to the enrichment of virus-specific CD8<sup>+</sup> T cells  
164 using MHC-I restricted antigens, CD4<sup>+</sup> T cells could also be enriched over 20-fold using MHC-II VIPR  
165 particles carrying a well validated CMV glycoprotein antigen (Fig. 1b).

166

167

168

169

170

171 *Optimization of antigen-specific micro aAPCs for T cell expansion*

172

173 Next we sought to optimize the design of the VIPR particle aAPCs to further enhance the expansion of  
174 antigen-specific T cells within the rapid 7-day stimulation culture. To this end, we first investigated  
175 the impact that the ratio of T cells to VIPR particles had on the proportion of CMV-specific T cells  
176 enriched at day-7. A dose-dependent enrichment was seen with lower doses of particles and higher  
177 numbers of T cells, such that an optimal enrichment was observed with a ratio of 20:1 T cells to VIPR  
178 particles (Fig. 1d). In addition, we observed that increasing the ratio of molecules of anti-CD28  
179 antibody to peptide-MHC-pentamer also increased the capacity of the VIPR particles for expansion of  
180 the antigen-specific VIL population (Fig. 1e)

181

182 *The detection and enrichment of SARS-CoV-2-specific T Cells in COVID-19 convalescent*  
183 *individuals*

184

185 We next evaluated whether VIPR particles can be used to enrich and expand SARS-CoV-2 specific T  
186 cells from COVID-19 patients. To investigate this, we obtained PBMCs from COVID-19 convalescent  
187 individuals 24 days or more after developing symptoms and testing positive by PCR, and analyzed the  
188 frequency and proportion of VIL specific for a recently published and validated immunodominant  
189 MHC-I SARS-CoV-2 epitope YLQPRFLL (YLQ)<sup>31</sup>. Surprisingly, we found YLQ antigen-specific VIL were  
190 barely detectible within the isolated T cell populations from these individuals (Fig. 2a&b).

191 However, after 7-day culture with MHC-I VIPR particles, antigen-specific CD8<sup>+</sup> T cells could be  
192 readily detected by pentamer staining and could be enriched and expanded to frequencies greater  
193 than 1% (Fig 2a&b). While the majority of PBMCs from convalescent individuals with the YLQ matched  
194 MHC allele (HLA A\*02), included T cells from which antigen specific VIL could be enriched, the overall  
195 frequency varied between individuals and did not appear to correlate with either the length of time  
196 since they were symptomatic, nor the reported severity of their symptoms (Fig. 2b)

197

198 *Rapid VIL expansion results in 1,000-fold enrichment of CMV antigen-specific T cells within 7-*  
199 *days*

200

201 Having demonstrated that VIPR particles can enrich both SARS-CoV-2 and CMV specific T cells, we  
202 evaluated the capacity for the 7-day culture system to expand the overall quantity of virus specific VIL.  
203 The T cell cultures were configured to include the same culturing conditions used in neoantigen TIL  
204 human clinical trials to enable rapid T cell expansion, thus in addition to the VIPR particles and high IL-

205 2 (6000 IU/ml), IL-7, IL-15 and NAC, T cells were cultured in Gas Permeable Rapid Expansion (G-REX)  
206 plates. These culture plates enable gas exchange from the base of the culture well, allowing cells to  
207 be cultured with a large ratio of media per surface area and abundant access to nutrients, and have  
208 been shown to facilitate a large and rapid expansion of primary human T cells<sup>32</sup>.

209 After 7-days of culture with VIPR particles, SARS-CoV-2 antigen-specific CD8<sup>+</sup> T cells could be  
210 robustly expanded in proportion, but most importantly in absolute quantity of T cells, to an average  
211 of over 1,000-fold (Fig. 2c). Thus, we found that cultures seeded with  $1 \times 10^6$  total CD3<sup>+</sup> T cells could  
212 reach expanded numbers, on average, between  $2.6 \times 10^7$  and  $4.5 \times 10^7$  total cells at day-7. This  
213 proliferative expansion coupled with the enrichment of the VIL population resulted in an average of  
214  $2.4 \times 10^5$  SARS-CoV-2 CD8<sup>+</sup> T cells per million CD3<sup>+</sup> cultured (Fig. 2c). A similar robustness in the  
215 expansion in absolute number of virus-specific CD8<sup>+</sup> VIL could also be observed with T cells from CMV-  
216 positive individuals when stimulated with MHC-I VIPR particles under these culture conditions (Fig.  
217 2d). After 7-days, antigen-specific CD8<sup>+</sup> T cells had increased from approximately  $2 \times 10^3$  cells to over  
218  $1.0 \times 10^6$ , leading to up to an average >700-fold expansion in cell number.

219 Collectively these data demonstrate the ability of the VIPR particle expansion protocol to  
220 rapidly enrich and expand VIL from low numbers in CMV-positive individuals and near undetectable  
221 numbers in COVID-19 convalescent individuals, to significantly large numbers of virus-specific T cells.

222

### 223 *The activation and T cell memory phenotype of rapidly-expanded CMV and SARS-CoV-2* 224 *antigen-specific VIL*

225

226 To evaluate the phenotype of SARS-CoV-2 specific T cells and CMV specific T cells that had undergone  
227 enrichment and expansion with VIPR particles, T cells were analyzed for expression of cell surface  
228 markers indicative of T cell activation. We observed SARS-CoV-2-specific CD8<sup>+</sup> T cells expressing co-  
229 stimulatory and activation markers 4-1BB, OX-40 and CD25, albeit variable between convalescent  
230 individuals, and an elevated expression of HLA-DR when compared to non-virus-specific T cells within  
231 the culture (Fig. 3a). The SARS-CoV-2 antigen-specific VIL population also showed a significant  
232 expression of the checkpoint markers PD-1, TIGIT, LAG-3, indicating these T cells have acquired a  
233 proliferative and activated functional phenotype (Fig. 3b). The same profile of activation marker and  
234 checkpoint gene expression was observed when CMV-specific VIL were stimulated after 7-day rapid  
235 expansion with VIPR particles, with a similarly observed variability between different CMV-positive  
236 individuals, indicating this culture platform is effective at rapid T cells expansion and activation with  
237 multiple viral antigens (Fig. 3c&d).

238 We analyzed the memory phenotype of the expanded SARS-CoV-2 and CMV virus-specific T  
239 cells by measuring expression of the canonical memory markers CD45RA and CD45RO and categorized  
240 the cell populations into either a naïve (CD45RO<sup>-</sup>, CD45RA<sup>+</sup>) or memory phenotype (CD45RO<sup>+</sup>, CD45RA<sup>-</sup>  
241 ). After the 7-day culture in IL-2, IL-7, IL-15 and NAC, the majority of CMV T cells had begun to adopt  
242 a memory phenotype, but the virus-specific CD8<sup>+</sup> T cells were almost exclusively expressing the  
243 highest levels of CD45RO and completely lost CD45RA expression, indicating the antigen-specific  
244 population had uniformly transitioned into memory T cells (Fig. 4a). Further delineation of the T cell  
245 memory phenotype by analysis of CD62L expression within the CD45RO<sup>+</sup> population revealed the  
246 virus-specific T cells had robustly differentiated into an effector memory T cell phenotype via  
247 downregulation of CD62L (Fig. 4a&b). The non-virus-specific T cells within these cultures however,  
248 consisted of significantly more naïve T cells. The same profile of effector memory T cells was observed  
249 when SARS-CoV-2-specific VIL were stimulated after 7-day rapid expansion with VIPR particles, again  
250 demonstrating the antigen-specific VIPR particle platform is effective at significantly expanding  
251 activated effector memory T cells over a short time-course. (Fig. 4c&d).

252

### 253 *Polyfunctional proinflammatory cytokine expression among rapidly-expanded CMV and SARS-* 254 *CoV-2 antigen-specific VIL*

255

256 To further evaluate the function of the rapidly expanded virus-specific VIL, we performed intracellular  
257 cytokine staining and flow cytometry and measured the proportion of the cells that were producing  
258 IFN $\gamma$ , TNF $\alpha$  and IL-2. VIPR particle expanded T cells from convalescent COVID-19 individuals were  
259 stimulated after 7-day culture with 20 $\mu$ g/ml of SARS-CoV-2 YLQPRTFLL peptide antigen for 6-hours.  
260 We observed strong expression of all three proinflammatory cytokines within the antigen-specific T  
261 cell population (identified by TCR specific pentamer staining), but could not detect expression of either  
262 IFN $\gamma$  or TNF $\alpha$  in the non-antigen-specific T cell population (T cells that do not bind the TCR-specific  
263 pentamer) nor within the T cells cultured for 7-days without any VIPR particle expansion (Fig. 5a&b).  
264 The antigen-specific T cells also showed significantly elevated levels of IL-2 when compared to the  
265 non-antigen specific CD8<sup>+</sup> population. When analyzed together we see an elevated proportion of cells  
266 expressing 1, 2 or all 3 cytokines in combination when compared to the non-SARS-CoV-2-specific T  
267 cells within the expanded culture (Fig. 5c&d).

268 The same functional response was observed with virus-specific VIL expanded in T cells isolated  
269 from CMV-positive individuals and stimulated for 6-hours with pp65 MHC-I epitope peptide antigen.  
270 Intracellular cytokine staining revealed a robust increase in production of all cytokines in the CMV-  
271 specific CD8<sup>+</sup> T cells when compared to the non-specific T cells from the same cultures or non-

272 stimulated controls (Fig. 5e&f). An elevated frequency of polyfunctional CD8<sup>+</sup> T cells expressing  
273 multiple proinflammatory cytokines was also seen in the CMV-specific T cell population (fig. 5g&h).

274 Taken together, these analyses demonstrate that elevated numbers of virus-specific VIL can  
275 be rapidly expanded in 7-days by VIPR particle culture and form robust activated, polyfunctional  
276 effector memory T cells.

277

## 278 DISCUSSION

279

280 Given the paucity of therapeutic options for the treatment of COVID-19 and the provocative data  
281 suggesting the importance of the immune T cell response to viral infections, we investigate a novel  
282 potential therapeutic modality to augment the anti-viral T cell response by providing a therapeutic  
283 immune boost of virus-specific T cells (VIL). Similar to adoptive cell therapy (ACT) methods in immuno-  
284 oncology to actively transfer Tumor Infiltrating Lymphocytes (TIL), here we demonstrate the potential  
285 utility of Virus Induced Lymphocytes (VIL) to deliver SARS-CoV-2 immunodominant viral antigens in  
286 the setting of nascent and acute COVID-19 infection. Unlike T cell immuno-oncology in which T cell  
287 expansion and subsequent efficacy requires substantial critical mass of quantity, and thus time, VIL  
288 serve a catalytic immune booster function and can be isolated and expanded *ex vivo* both autologously  
289 and also MHC typed for allogenic delivery in a 7-day vein-to-vein time which is clinically practical and  
290 relevant (as depicted in fig. 6a).

291 In the setting of COVID-19 pathogenesis, studies have found individuals suffering from a more  
292 severe presentation of the disease typically require a duration of hospitalization ranging from 5 to 29  
293 days<sup>33, 34</sup>. Thus, a therapeutic treatment to improve patient outcome must be rapidly administered  
294 during the critical time window of disease progression prior to and/or early in the patient's intubation  
295 and ventilatory support. Herein lies the opportunity for a T cell therapy that can robustly expand the  
296 quantity and quality of virus-reactive T cells within this short duration to help boost the immune  
297 response and potentiate the patient's own *in vivo* T cell response to the viral infection. Developments  
298 in Rapid Expansion Protocols (REP) for T cell and TIL expansion in the setting of clinical oncology have  
299 enabled methods for the robust and exponential *ex vivo* expansion of unenriched, as well as  
300 neoantigen-enriched, T cells for the autologous treatment of solid tumors<sup>35, 36, 37, 38</sup>. In fact, large  
301 quantities of antigen-specific TIL can be expanded in just 22 days using well established protocols<sup>39</sup>.  
302 This duration is however too long for a clinically relevant cell therapy in the setting of COVID-19 and  
303 thus in this study we have developed a more rapid T cell expansion protocol that builds upon the  
304 principles of TIL and T cell REP.

305 Our approach enables an over 1,000-fold expansion in the numbers of viral antigen-specific  
306 T cells in just 7-days from isolation of a patient's T cells, providing a higher quantity of activated,  
307 polyfunctional effector memory cells. This study demonstrates the antigen-specific expansion of  
308 SARS-CoV-2 T cells from convalescent COVID-19 patients to demonstrate applicability for this viral  
309 pathogen, yet one important consideration is that these individuals have very low numbers of  
310 recirculating SARS-CoV-2 specific T cells in their blood due to the timeframe since their infection and  
311 recovery (fig. 2b). Hospitalized, symptomatic COVID-19 patients with a severe form of the disease will  
312 be undergoing a significant cellular immune response whereby the numbers of virus-specific T cells  
313 may have expanded, even if overall T cell numbers may be reduced in some individuals<sup>40</sup>. While this  
314 T cell response needs therapeutically boosting to potentiate viral clearance and ensure positive  
315 disease outcome, we expect a more robust and significantly elevated VIL expansion can be achieved  
316 when T cells are acquired from suffering COVID-19 patients as opposed to recovered convalescent  
317 individuals. When considering the translation of this platform into the clinic as a potential cell therapy  
318 for hospitalized COVID-19 patients, based on the level of enrichment and expansion demonstrated in  
319 this study, and a prediction of the number of SARS-COV-2 cells in the blood of COVID-19 individuals,  
320 we calculate an estimated capability to expand and deliver an average of approximately  $3.5 \times 10^9$  SARS-  
321 CoV-2 CD8<sup>+</sup> and/or CD4<sup>+</sup> T cells back to the patient within 7-days (Fig. 6b).

322 The key features of this VIL expansion platform include the use of high concentration of IL-2  
323 to enable robust T cell proliferation supported by IL-7 and IL-15, and the addition of N-acetyl cysteine  
324 (NAC) which has been shown to significantly reduce upregulation of the DNA damage marker  $\gamma$ H2AX,  
325 and the subsequent cell death seen in T cell culturing<sup>41</sup>. The expansion of VIL in G-REX plates and  
326 flasks also improves overall T cell proliferation by supporting more effective gaseous exchange and  
327 nutrient availability, further adding to the rapidity by which significant numbers of virus-specific VIL  
328 can be generated (Fig. 2c&d). A major component and innovation of the platform are the VIPR  
329 Particles themselves, which provide a viral epitope peptide in the context of MHC class I pentamers,  
330 or class II tetramers, to bind and stimulate the cognate TCRs specific for this antigen (fig. 1a). These  
331 aAPCs mimic the physiological presentation of viral antigens to CD8<sup>+</sup> T cells by dendritic cells that  
332 occurs in local draining lymph nodes during viral infection, and the coating of the particles with anti-  
333 CD28 antibodies provides the necessary co-stimulatory signals that are critically required for effective  
334 T cell activation and formation of effector memory T cells<sup>42</sup>. It is well established that costimulatory  
335 signals like those delivered by CD28 (signal two) dictate whether CD8<sup>+</sup> T cells will become optimally  
336 activated and expand, or whether the activation will be suboptimal<sup>42</sup>. While studies have also shown  
337 that T cells can indeed be expanded, from memory, and protect from viral infections in animal models  
338 in the absence of co-stimulation<sup>43,44</sup>, it was found that very high levels of TCR stimulation were needed



339 to overcome the need for co-stimulation<sup>45, 46</sup>. Thus, if a strong, shared, immunodominant and well  
340 validated peptide antigen is known and available for a viral pathogen, large numbers of VIL could  
341 potentially be expanded *ex vivo* by soluble peptide in the absence of an aAPC or co-stimulation.  
342 However, this situation is clinically irrelevant for most pathogens whereby multiple immunogenic  
343 epitopes typically exist and the comparative affinity for their cognate TCRs may not be known (as in  
344 an emerging pandemic). This is true in the case for the recently emerged SARS-CoV-2 virus which has  
345 been shown to harbor dozens of immunogenic shared epitopes spread throughout the genome, 90%  
346 of which are not located in the spike protein and show almost no cross-reactivity with known epitopes  
347 in seasonal coronaviruses, and for which T cell immunity must be established empirically<sup>12, 31</sup>.

348 Furthermore, a hospitalized COVID-19 patient's own TCR repertoire for SARS-CoV-2 cannot be  
349 quickly assessed and determined to ensure they can respond to the strongest of these peptide  
350 epitopes in the absence of co-stimulation. Thus, VIL expansion platforms for newly emerged  
351 pathogens, as well as seasonal variants of existing viruses, will benefit from aAPC-mediated  
352 approaches, where the presence of CD28 co-stimulation should lower the T cell activation threshold  
353 and provide robust co-stimulation to ensure strong proliferation and effector memory T cell  
354 formation.

355 An alternative approach for VIL expansion by viral antigen presentation to T cells in the  
356 context of this co-stimulation, is the use of autologous professional antigen presentation cells (APCs)  
357 such as dendritic cells harvested from the patient's blood, pulsed with antigenic peptide and co-  
358 cultured with the T cells. While in theory this works well for antigen-specific activation and expansion  
359 of CD8<sup>+</sup> and CD4<sup>+</sup> T cells and is routinely used in the setting of neoantigen-specific TIL expansion<sup>38</sup>, this  
360 is impractical in the setting of rapid VIL expansion as a therapeutic for hospitalized patients suffering  
361 from acute viral infections such as with SARS-CoV-2. Dendritic cells are typically generated from  
362 autologous monocytes through a series of *ex vivo* maturation steps with different cytokines which  
363 includes approximately 6 days of culture in IL-4 and GM-CSF to generate immature DCs before further  
364 maturation<sup>47</sup>. This requirement for several days of manipulation before the dendritic cells can be used  
365 to activate and expand the patient's VIL, precludes their use for rapid T cell expansion in the setting  
366 of acute and severe viral infections such as with COVID-19. Therefore, we believe the VIPR platform  
367 based on artificial APCs offers a clinically meaningful and practical alternative to this approach.

368 Given the importance of the aAPC VIPR particles for T cell stimulation, we optimized the  
369 design to maximize the strength of the TCR and CD28 engagement by determining both the effective  
370 dose ratio of particles per T cell (1:20) and the optimal density of peptide-MHC-pentamer versus anti-  
371 CD28 antibody (1:30) on the surface of the particle (fig. 1d&e). When the optimized VIPR particles  
372 were combined with other elements of the protocol, including high cytokine concentrations and G-

373 REX flasks, we thus observed not only a significant expansion in virus-specific VIL cell numbers (Fig.  
374 2c&d), but that these cells had developed into activated effector memory T cells (Figs. 3&4). This was  
375 crucial to establish a pool of virus-reactive T cells that can not only mount a primary immune response  
376 against the virus when adoptively transferred to the patient, but also engender immunological  
377 memory to ensure the duration of the response is long lasting. Given the active state of the VIL by  
378 day-7, it is likely that further cellular expansion will be catalyzed upon ACT to the patient given the  
379 characteristic upregulated endogenous inflammasome of COVID-19 patients. Importantly, after a 7-  
380 day expansion of the SARS-CoV-2 VIL, the cells were producing robust levels of polyfunctional cytokine  
381 (Fig. 5). Thus, the expanding virus-specific VIL that can subsequently be transferred back to the patient  
382 are primed to mount a functional cellular response in the context of cytokine release and recruitment  
383 of other immune cells. These antigen-specific CD8<sup>+</sup> T cells are also likely primed to recognize and  
384 mount a cytolytic response against infected cells, aiding to clear the viral infection.

385 The VIPR rapid expansion platform is modular and tunable to multiple viral antigens restricted  
386 to different MHC alleles. Using validated CMV epitopes, we generated MHC class II VIPR particles  
387 against the DRB1\*07:01 restricted gB 215-229 antigen and were able to enrich and expand CD4<sup>+</sup> T  
388 cells (Fig. 1b). Thus, this technology can be used to expand both T Helper and Cytolytic virus-specific  
389 VIL to provide a modality to tune a specific cell therapy product to treat different viral diseases. The  
390 enrichment and expansion of CMV-specific T cells demonstrates the flexibility of the VIPR particle  
391 system for addressing cell therapies for diverse pathogens where immunogenic epitopes are known.  
392 VIPR particles are off-the-shelf reagents that can be rapidly utilized for *ex vivo* T cell expansion in the  
393 clinic without any additional manufacturing lead time. We expect that this technology would provide  
394 a modality for expansion of all clinically relevant virally-mediated diseases where an immune boosting  
395 dose of virus-specific T cells would aid in viral clearance and disease outcome. Furthermore, due to  
396 the immune catalytic nature of T cells and their ability to expand further *in vivo* and recruit additional  
397 cells of the immune system, we believe that an efficacious therapeutic dose of virus-specific T is likely  
398 to be well within the numbers achievable within short durations of expansion. In instances whereby  
399 such a short duration of T cell expansion is not as critical as required in diseases like COVID-19, this  
400 technology can also enable the expansion and cryopreservation of virus-specific VIL.

401 To be broadly applicable as a pragmatic modality that is scalable, we have MHC typed donor  
402 pools of SARS-CoV-2-specific VIL for use as an allogeneic off-the-shelf therapy at scale. In this setting,  
403 these T cells are tissue matched to COVID-19 patients and provided as an allogeneic cell therapy  
404 product to combat an active infection. Thus, by virtue of having pre-expanded stocks of SARS-COV-2  
405 cells from SARS-CoV-2 donors, hospitalized patients can be treated immediately with the cells within  
406 the ICU upon MHC tissue type results. Furthermore, cryopreservation of other VIL, such as MHC -



407 typed CMV-specific VIL, could, as an example, be used to immunize bone marrow transplant recipients  
408 or other immunocompromised individuals against adventitious pathogens<sup>48</sup>.

409 In summary we demonstrate a novel technology platform for the robust and rapid expansion  
410 of virus-specific T cells as a potential cell therapy for COVID-19 and other viral pathogens. Heretofore,  
411 the promising antigen-specific therapeutic approaches to date, including polyclonal antibody cocktails  
412 and monoclonal antibodies, and current prophylactic vaccine approaches to COVID-19, all have been  
413 focused on neutralizing antibodies. However, complete immune protection is likely also a function of  
414 the long-lasting central memory T cell response to provide both cellular immunity, and potentiate  
415 humoral immunity, and thus prolong the duration of protection<sup>8, 11</sup>.

416 As development and validation of the VIL platform continues, a global “second-wave” of  
417 COVID-19 morbidity and mortality, perhaps exacerbated by seasonal inflection, appears to be  
418 accelerating<sup>49</sup>. Validated therapies are few and largely supportive or non-specific, such as the use of  
419 dexamethasone to delay mechanical ventilation in COVID-19 induced pulmonary failure. The  
420 morbidity and mortality of COVID-19 critical illness remain alarmingly high<sup>50</sup>. Thus, there is an urgent  
421 need for specificity and efficacy in the clinic to mitigate disease progression and severity. Using the  
422 same cGMP validation processes employed in the setting of a CRISPR-engineered TIL cell therapy for  
423 cancer, we will explore a timely regulatory path to evaluating the VIL platform technology in a phase  
424 I/II clinical trial of SARS-CoV-2 -infected patients, should there continue to be an urgent need during  
425 the course of the COVID-19 pandemic.

426

## 427 **METHODS**

428

### 429 *Patient samples and preparation of T cells*

430 Peripheral blood mononuclear cells were obtained from anonymized CMV-positive individuals and  
431 convalescent COVID-19 individuals (Caltag Medsystems, Tissue Solutions Ltd, Precision for Medicine,  
432 Inc.) and obtained, handled and stored in accordance with the Human Tissue Authority UK regulations.  
433 Genomic DNA was extracted from PBMC samples using the Genra Puregene DNA isolation kit  
434 (Qiagen) and DNA samples were HLA-typed by sequencing at Class I (HLA-A, -B & -C) and Class II (HLA-  
435 DRB1) loci (MC Diagnostics). Total CD3<sup>+</sup> T cells were isolated from unfractionated PBMCs using the  
436 EasySep™ Human T Cell Isolation Kit (Stem Cell Technologies) with a DynaMag™-2 magnet  
437 (ThermoFisher Scientific) according to the manufacturer’s guidelines. Purity and viability of isolated T  
438 cells was assessed using flow cytometry prior to cryopreservation of isolated T cells in CryoStore CS10  
439 cryopreservation media (Stem Cell Technologies) at a density of 1-1.5x10<sup>7</sup> cells per ml.

440

#### 441 *Preparation of VIPR Particles*

442 Micro-aAPC VIPR particles were constructed by direct conjugation of biotin labelled peptide-MHC-  
443 Pentamers and biotinylated MHC class II Tetramers to streptavidin Dynabeads in combination with  
444 biotinylated anti-CD28 antibodies. Pro5 MHC Class I Pentamers were provided by ProImmune Ltd and  
445 include the following peptide epitopes: CMV pp65 HLA A\*02:01-restricted NLVPMVATV epitope;  
446 SARS-CoV-2 Spike protein 269-277 HLA A\*02:01-restricted YLQPRTFLL epitope. ProM2 MHC class II  
447 biotinylated Monomers were also obtained from ProImmune for the DRB1\*07:01-restricted CMV gB  
448 215-229 PDDYSNTHSTRYVTV epitope. These biotin-labelled MHC-peptide Pentamers and biotinylated  
449 MHC-peptide Monomer complexes, and mouse anti-human CD28 antibody (BD Biosciences) were  
450 conjugated to M270 Streptavidin Dynabeads (Thermo Scientific) at defined molar ratios of  
451 Pentamer:anti-CD28 and Monomer:anti-CD28 (calculated to account for tetramer formation of these  
452 monomers), and both in molar excess of the number of streptavidin molecules per Dynabead. Bead-  
453 conjugation was carried out at 4°C in Phospho-buffered saline (PBS, Gibco), for 1 hour with regular  
454 agitation. Conjugated VIPR particles were centrifuged at 14,500 xg for 3 minutes at 4°C and washed  
455 three times in PBS while the beads were immobilized in an Invitrogen DynaMag-2 magnet (Thermo  
456 Scientific). VIPR particles were resuspended in sterile PBS at a concentration of 5x10<sup>8</sup> particles per ml  
457 and stored at 4°C.

458

#### 459 *Expansion of antigen-specific T cells by VIPR particles*

460 Isolated human CD3<sup>+</sup> T cells were cultured in X-VIVO-15 Basal Media (Lonza) supplemented with 10%  
461 Human AB Serum Heat Inactivated (Sigma), 6000IU/ml Recombinant Human IL-2 (Peprotech), 5ng/ml  
462 Recombinant Human IL-7 (Peprotech), 5ng/ml Recombinant Human IL-15 (Peprotech) and 10mM N-  
463 Acetyl-L-cysteine (Sigma). T cells were seeded at a density of 2x10<sup>5</sup> cells per well of U-bottom 96-well  
464 plates, or at a density of 1-2x10<sup>6</sup> T cells per cm<sup>2</sup> of G-REX 24-well plates (Wilson-Wolf). At the time of  
465 T cell seeding, VIPR particles were added to the relevant samples at a ratio of 20 T cells per particle,  
466 and cells were cultured for 7-days in a 37°C, 5% CO<sub>2</sub> culture incubator. In addition, a sample of the T  
467 cells was also analyzed by flow cytometry at Day-0 to measure the starting proportion of antigen-  
468 specific T cells (see methods below). For some cultures the media was replaced every 2-3 days with  
469 fresh complete media including cytokines and NAC (but no extra addition of VIPR particles) and media  
470 in G-REX cultures was left unchanged for the duration of 7-days in some experiments to promote cell  
471 expansion. On day 7, T cell numbers were assessed by harvesting all cells, washing in PBS followed by  
472 centrifugation at 300 xg for 10 minutes and then counting using a CellDrop Automated Cell Counter  
473 (DeNovix). The proportion of expanded antigen-specific T cells was assessed at Day-7 by flow  
474 cytometry.

475 *Flow cytometry analysis of T cell phenotype*

476 For flow cytometric analysis of the antigen-specific T cell population and cell surface marker  
477 expression, cells were harvested from culture plates and washed using PBS with 1% Bovine Serum  
478 Albumen (Thermo Scientific) and were then stained with monoclonal antibodies specific for CD8  
479 (HIT8A, 1:100), CD4 (OKT4, 1:100), HLA-DR (L243 1:80), LAG-3 (11C3C65, 1:80), TIGIT (VSTM3, 1:40),  
480 CD45RO (UCHL1, 1:40), CD45RA (HI100, 1:80), TIM3 (F38-2E2, 1:40), CD62L (DREG-56, 1:40), CD57  
481 (QA17A04, 1:80), PD-1 (EH12.1, 1:40), OX-40 (Ber-ACT35, 1:40), CD25 (MA2-51, 1:40), 41BB (4B4-1,  
482 1:40), (Biolegend) or specific for CD8 (RPA-T8, 1:100) (BD Bioscience), or TNF- $\alpha$  (MAb11, 1:40) and CD3  
483 (UCHT1, 1:100) (ThermoFisher). CMV pp65 and SARS-CoV-2 Spike antigen-specific T cells were  
484 detected by staining cells with R-PE-labelled Pro5 Pentamers (ProImmune, Ltd), and CMV gB215-229  
485 specific T cells stained with R-PE labelled ProT2 Tetramer for 20 minutes at room temperature  
486 according to manufacturer's recommendation. Live/Dead Fixable Dead Cell Stains (Invitrogen) or  
487 SYTOX Blue Dead Cell Stain (Invitrogen) were included in all experiments to exclude dead cells. After  
488 staining, cells were resuspended in PBS with 2% Human Heat Inactivated AB Serum (Sigma) and 0.1M  
489 EDTA pH 8.0 (Invitrogen) before analysis on a Fortessa flow cytometer (BD Bioscience) and data  
490 analyzed using FlowJo 10 software (BD Biosciences).

491

492 *Intracellular cytokine staining*

493 After 7-days of expansion with VIPR particles, the T cell cultures were stimulated for 6 hours with  
494 20 $\mu$ g/ml peptide antigen (>95% purity) specific for the VIPR particle expanded CD8<sup>+</sup> population (CMV  
495 pp65: NLVPMVATV; SARS-CoV-2 S protein 269-277 YLQPRTFLL), all peptides were synthesized and  
496 obtained from ProImmune, Ltd. After 1-hour of peptide stimulation, GolgiStop solution was added  
497 (containing Monensin protein transport inhibitor) to block intracellular protein transport (BD  
498 Bioscience). As a positive control for cytokine production, T cells were also stimulated for 6 hours  
499 with 50ng/ml PMA and 1 $\mu$ g/ml Ionomycin (Sigma). T cells were then harvested, and cells fixed and  
500 permeabilized using BD Cytofix/Cytoperm Fixation/Permeabilization Solution (ThermoFisher). Cells  
501 were then stained for surface markers followed by intracellular cytokines using antibodies specific for  
502 IFN- $\gamma$  (4S.B3, 1:40) (Biolegend) IL-2 (MQ1-17H12, 1:40) (BD Bioscience), or TNF- $\alpha$  (MAb11, 1:40)  
503 (ThermoFisher). Flow analysis was carried out on a Fortessa flow cytometer (BD Bioscience) and data  
504 analyzed using FlowJo 10 software (BD Biosciences).

505

506

507

508

509 *Statistical analyses*

510 Statistical differences between two sample groups, where appropriate, was analyzed by a standard  
511 Student's two-tailed, non-paired, t test using GraphPad Prism Software version 8. P values are  
512 included in the figures where statistical analyses have been carried out.

513

514 Ethics declarations

515

516 D.B. has a sponsored research collaboration funded by Intima Bioscience. Intima Bioscience has  
517 patents filed based on the findings described herein. The authors declare no competing interests.

518

519 **REFERENCES**

520

521 1. Stevanovic, S. *et al.* Complete regression of metastatic cervical cancer after treatment with  
522 human papillomavirus-targeted tumor-infiltrating T cells. *J Clin Oncol* **33**, 1543-1550 (2015).

523

524 2. Tran, E. *et al.* Cancer immunotherapy based on mutation-specific CD4+ T cells in a patient  
525 with epithelial cancer. *Science* **344**, 641-645 (2014).

526

527 3. Zacharakis, N. *et al.* Immune recognition of somatic mutations leading to complete durable  
528 regression in metastatic breast cancer. *Nat Med* **24**, 724-730 (2018).

529

530 4. Lee, H.J. *et al.* Expansion of tumor-infiltrating lymphocytes and their potential for application  
531 as adoptive cell transfer therapy in human breast cancer. *Oncotarget* **8**, 113345-113359 (2017).

532

533 5. Schmidt, M.E. & Varga, S.M. The CD8 T Cell Response to Respiratory Virus Infections. *Front*  
534 *Immunol* **9**, 678 (2018).

535

536 6. Cox, M.A., Kahan, S.M. & Zajac, A.J. Anti-viral CD8 T cells and the cytokines that they love.  
537 *Virology* **435**, 157-169 (2013).

538

539 7. Wherry, E.J. & Ahmed, R. Memory CD8 T-cell differentiation during viral infection. *J Virol* **78**,  
540 5535-5545 (2004).

541

542 8. Radziewicz, H., Uebelhoer, L., Bengsch, B. & Grakoui, A. Memory CD8+ T cell differentiation  
543 in viral infection: a cell for all seasons. *World J Gastroenterol* **13**, 4848-4857 (2007).

544

545 9. Le Bert, N. *et al.* SARS-CoV-2-specific T cell immunity in cases of COVID-19 and SARS, and  
546 uninfected controls. *Nature* **584**, 457-462 (2020).

547

548 10. Barrett, A.J., Prockop, S. & Bollard, C.M. Virus-Specific T Cells: Broadening Applicability. *Biol*  
549 *Blood Marrow Transplant* **24**, 13-18 (2018).

550

551 11. Peng, Y. *et al.* Broad and strong memory CD4(+) and CD8(+) T cells induced by SARS-CoV-2 in  
552 UK convalescent individuals following COVID-19. *Nat Immunol* **21**, 1336-1345 (2020).

553

- 554 12. Ferretti, A.P. *et al.* Unbiased Screens Show CD8(+) T Cells of COVID-19 Patients Recognize  
555 Shared Epitopes in SARS-CoV-2 that Largely Reside outside the Spike Protein. *Immunity* (2020).  
556
- 557 13. Chen, Z. & John Wherry, E. T cell responses in patients with COVID-19. *Nat Rev Immunol* **20**,  
558 529-536 (2020).  
559
- 560 14. Kroemer, M. *et al.* COVID-19 patients display distinct SARS-CoV-2 specific T-cell responses  
561 according to disease severity. *J Infect*, 4816 (2020).  
562
- 563 15. Callaway, E. The race for coronavirus vaccines: a graphical guide. *Nature* **580**, 576-577  
564 (2020).  
565
- 566 16. Mercado, N.B. *et al.* Single-shot Ad26 vaccine protects against SARS-CoV-2 in rhesus  
567 macaques. *Nature* **586**, 583-588 (2020).  
568
- 569 17. Folegatti, P.M. *et al.* Safety and immunogenicity of the ChAdOx1 nCoV-19 vaccine against  
570 SARS-CoV-2: a preliminary report of a phase 1/2, single-blind, randomised controlled trial. *Lancet*  
571 **396**, 467-478 (2020).  
572
- 573 18. Anderson, E.J. *et al.* Safety and Immunogenicity of SARS-CoV-2 mRNA-1273 Vaccine in Older  
574 Adults. *N Engl J Med* (2020).  
575
- 576 19. Walsh, E.E. *et al.* Safety and Immunogenicity of Two RNA-Based Covid-19 Vaccine  
577 Candidates. *N Engl J Med* (2020).  
578
- 579 20. Zhu, F.C. *et al.* Immunogenicity and safety of a recombinant adenovirus type-5-vectored  
580 COVID-19 vaccine in healthy adults aged 18 years or older: a randomised, double-blind, placebo-  
581 controlled, phase 2 trial. *Lancet* **396**, 479-488 (2020).  
582
- 583 21. Logunov, D.Y. *et al.* Safety and immunogenicity of an rAd26 and rAd5 vector-based  
584 heterologous prime-boost COVID-19 vaccine in two formulations: two open, non-randomised phase  
585 1/2 studies from Russia. *Lancet* **396**, 887-897 (2020).  
586
- 587 22. Xia, S. *et al.* Safety and immunogenicity of an inactivated SARS-CoV-2 vaccine, BBIBP-CorV: a  
588 randomised, double-blind, placebo-controlled, phase 1/2 trial. *Lancet Infect Dis* (2020).  
589
- 590 23. Xia, S. *et al.* Effect of an Inactivated Vaccine Against SARS-CoV-2 on Safety and  
591 Immunogenicity Outcomes: Interim Analysis of 2 Randomized Clinical Trials. *JAMA* **324**, 951-960  
592 (2020).  
593
- 594 24. Keech, C. *et al.* Phase 1-2 Trial of a SARS-CoV-2 Recombinant Spike Protein Nanoparticle  
595 Vaccine. *N Engl J Med* (2020).  
596
- 597 25. Seow, J. *et al.* Longitudinal observation and decline of neutralizing antibody responses in the  
598 three months following SARS-CoV-2 infection in humans. *Nat Microbiol* (2020).  
599
- 600 26. Investigational COVID-19 Convalescent Plasma. [https://www.fda.gov/regulatory-](https://www.fda.gov/regulatory-information/search-fda-guidance-documents/investigational-covid-19-convalescent-plasma)  
601 [information/search-fda-guidance-documents/investigational-covid-19-convalescent-plasma](https://www.fda.gov/regulatory-information/search-fda-guidance-documents/investigational-covid-19-convalescent-plasma) (2020).  
602

- 603 27. A Study of Metastatic Gastrointestinal Cancers Treated With Tumor Infiltrating Lymphocytes  
604 in Which the Gene Encoding the Intracellular Immune Checkpoint CISH Is Inhibited Using CRISPR  
605 Genetic Engineering. <https://clinicaltrials.gov/ct2/show/NCT04426669> (2020).  
606
- 607 28. Marthandan, S., Hyland, P., Pawelec, G. & Barnett, Y. An investigation of the effects of the  
608 antioxidants, ebselen or N-acetyl cysteine on human peripheral blood mononuclear cells and T cells.  
609 *Immun Ageing* **10**, 7 (2013).  
610
- 611 29. Kern, F. *et al.* Cytomegalovirus (CMV) phosphoprotein 65 makes a large contribution to  
612 shaping the T cell repertoire in CMV-exposed individuals. *J Infect Dis* **185**, 1709-1716 (2002).  
613
- 614 30. Hyun, S.J. *et al.* Comprehensive Analysis of Cytomegalovirus pp65 Antigen-Specific CD8(+) T  
615 Cell Responses According to Human Leukocyte Antigen Class I Allotypes and Intraindividual  
616 Dominance. *Front Immunol* **8**, 1591 (2017).  
617
- 618 31. Shomuradova, A.S. SARS-CoV-2 epitopes are recognized by a public and diverse repertoire of  
619 human T cell receptors. *Immunity in press* (2020).  
620
- 621 32. Vera, J.F. *et al.* Accelerated production of antigen-specific T cells for preclinical and clinical  
622 applications using gas-permeable rapid expansion cultureware (G-Rex). *J Immunother* **33**, 305-315  
623 (2010).  
624
- 625 33. Rees, E.M. *et al.* COVID-19 length of hospital stay: a systematic review and data synthesis.  
626 *BMC Med* **18**, 270 (2020).  
627
- 628 34. Vultaggio, A. *et al.* Prompt Predicting of Early Clinical Deterioration of Moderate-to-Severe  
629 COVID-19 Patients: Usefulness of a Combined Score Using IL-6 in a Preliminary Study. *J Allergy Clin*  
630 *Immunol Pract* **8**, 2575-2581 e2572 (2020).  
631
- 632 35. Jin, J. *et al.* Simplified method of the growth of human tumor infiltrating lymphocytes in gas-  
633 permeable flasks to numbers needed for patient treatment. *J Immunother* **35**, 283-292 (2012).  
634
- 635 36. Dudley, M.E., Wunderlich, J.R., Shelton, T.E., Even, J. & Rosenberg, S.A. Generation of tumor-  
636 infiltrating lymphocyte cultures for use in adoptive transfer therapy for melanoma patients. *J*  
637 *Immunother* **26**, 332-342 (2003).  
638
- 639 37. Douglas C. Palmer, B.R.W., Yogin Patel, Matthew J. Johnson, Christine M. Kariya, Walker S.  
640 Lahr, Maria R. Parkhurst, Jared J Gartner, Todd D Prickett, Frank J. Lowery, Rigel J. Kishton, Devikala  
641 Gurusamy, Zulmarie Franco, Suman K. Vodnala, Miechaleen D. Diers, Natalie K. Wolf, Nicholas J.  
642 Slipek, David H. McKenna, Darin Sumstad, Lydia Viney, Tom Henley, Tilmann Bürckstümmer, Oliver  
643 Baker, Ying Hu, Chunhua Yan, Daoud Meerzaman, Kartik Padhan, Winnie Lo, Parisa Malekzadeh, Li  
644 Jia, Drew C. Deniger, Shashank J. Patel, Paul F. Robbins, R. Scott McIvor, Modassir Choudhry, Steven  
645 A. Rosenberg, Branden S. Moriarity, Nicholas P. Restifo. Internal checkpoint regulates T cell  
646 neoantigen reactivity and susceptibility to PD1 blockade. *bioRxiv In press* (2020).  
647
- 648 38. Bianchi, V., Harari, A. & Coukos, G. Neoantigen-Specific Adoptive Cell Therapies for Cancer:  
649 Making T-Cell Products More Personal. *Front Immunol* **11**, 1215 (2020).  
650
- 651 39. Amod Sarnaik, N.I.K., Jason Alan Chesney, Harriet M. Kluger, Brendan D. Curti, Karl D. Lewis,  
652 Sajeve Samuel Thomas, Eric D. Whitman, Omid Hamid, Jose Lutzky, Anna C. Pavlick, Jeffrey S. Weber,  
653 James M.G. Larkin, Debora Barton, Lotus Yung, Sam Suzuki, Maria Fardis, and John M. Kirkwood.



- 654 Safety and efficacy of cryopreserved autologous tumor infiltrating lymphocyte therapy (LN-144,  
655 lifileucel) in advanced metastatic melanoma patients who progressed on multiple prior therapies  
656 including anti-PD-1. *Journal of Clinical Oncology* **37**, 2518-2518 (2019).  
657
- 658 40. Diao, B. *et al.* Reduction and Functional Exhaustion of T Cells in Patients With Coronavirus  
659 Disease 2019 (COVID-19). *Front Immunol* **11**, 827 (2020).  
660
- 661 41. Scheffel MJ, S.G., Simms P, Garrett-Mayer E, Mehrotra S, Nishimura MI, Voelkel-Johnson C.  
662 Efficacy of Adoptive T-cell Therapy Is Improved by Treatment with the Antioxidant N-Acetyl Cysteine,  
663 Which Limits Activation-Induced T-cell Death. *Cancer Res* **15**, 6006-6016 (2016).  
664
- 665 42. Boesteanu, A.C. & Katsikis, P.D. Memory T cells need CD28 costimulation to remember.  
666 *Semin Immunol* **21**, 69-77 (2009).  
667
- 668 43. Shahinian, A. *et al.* Differential T cell costimulatory requirements in CD28-deficient mice.  
669 *Science* **261**, 609-612 (1993).  
670
- 671 44. Suresh, M. *et al.* Role of CD28-B7 interactions in generation and maintenance of CD8 T cell  
672 memory. *J Immunol* **167**, 5565-5573 (2001).  
673
- 674 45. Kundig, T.M. *et al.* Duration of TCR stimulation determines costimulatory requirement of T  
675 cells. *Immunity* **5**, 41-52 (1996).  
676
- 677 46. Viola, A. & Lanzavecchia, A. T cell activation determined by T cell receptor number and  
678 tunable thresholds. *Science* **273**, 104-106 (1996).  
679
- 680 47. Hopewell, E.L. & Cox, C. Manufacturing Dendritic Cells for Immunotherapy: Monocyte  
681 Enrichment. *Mol Ther Methods Clin Dev* **16**, 155-160 (2020).  
682
- 683 48. Nelson, A.S. *et al.* Virus-specific T-cell therapy to treat BK polyomavirus infection in bone  
684 marrow and solid organ transplant recipients. *Blood Adv* **4**, 5745-5754 (2020).  
685
- 686 49. Thompson, C.N. *et al.* COVID-19 Outbreak - New York City, February 29-June 1, 2020.  
687 *MMWR Morb Mortal Wkly Rep* **69**, 1725-1729 (2020).  
688
- 689 50. Tomazini, B.M. *et al.* Effect of Dexamethasone on Days Alive and Ventilator-Free in Patients  
690 With Moderate or Severe Acute Respiratory Distress Syndrome and COVID-19: The CoDEX  
691 Randomized Clinical Trial. *JAMA* **324**, 1307-1316 (2020).  
692  
693  
694  
695  
696  
697  
698  
699  
700

701 **Fig. 1: Detection and enrichment of antigen-specific Virus Induced Lymphocytes (VIL) in CMV**  
702 **infected individuals. a,** Strategy for the isolation, stimulation and enrichment of CMV antigen-specific  
703 T cells from donor PBMCs. **b,** Representative flow-cytometric analysis showing proportions of antigen-  
704 specific CD8<sup>+</sup> and CD4<sup>+</sup> T cells identified by Pentamer staining, 7-days after enrichment and expansion  
705 with antigen-specific VIPR Particles. **c,** Summary of CD8<sup>+</sup> data obtained in b, (*n*=3). **d,** Histogram plot  
706 showing this VIL enrichment is VIPR particles dose-dependent (*n*=3). **e,** Histogram showing impact on  
707 VIL enrichment of MHC-I pentamer and anti-CD28 ratio conjugated to VIPR particles (*n*=3).

708

709 **Fig. 2: Rapid VIL expansion results in a 1,000-fold enrichment of SARS-CoV-2 antigen-specific T cells**  
710 **within 7-days from convalescent donors. a,** Representative flow-cytometric analysis showing  
711 proportions of SARS-CoV-2 antigen-specific CD8<sup>+</sup> T cells 7-days after expansion and enrichment with  
712 YLQPRTFL antigen-specific VIPR Particles. **b,** Table describing the clinical presentation of convalescent  
713 COVID-19 donors used in this study and the proportions of SARS-CoV-2 specific VIL detectible before  
714 enrichment, and fold expansion by VIPR particles. **c,** Summary of CD8<sup>+</sup> SARS-CoV-2 VIL %, cell number  
715 and fold change after VIPR expansion (*n*=7). **d,** Histograms showing total CMV pp65 antigen-specific  
716 CD8<sup>+</sup> T cell numbers expanded by VIPR particles after 7-days and overall fold change in antigen specific  
717 cells (*n*=3).

718

719 **Fig. 3: The activation and exhaustion phenotype of rapidly-expanded SARS-CoV-2 and CMV antigen-**  
720 **specific VIL. a,** Expression of activation markers, 4-1BB, OX-40, CD25 and HLA-DR, and **b,** expression  
721 of checkpoint genes PD-1, LAG-3 and TIGIT among enriched and expanded SARS-CoV-2-specific CD8<sup>+</sup>  
722 T cells at day 7 (*n*=8). **c,** Analysis as in a, for CMV-specific CD8<sup>+</sup> T cells and **d,** Analysis as in b, for CMV-  
723 specific CD8<sup>+</sup> T cells (*n*=4).

724

725 **Fig. 4: The T cell memory phenotype of rapidly-expanded CMV and SARS-CoV-2 antigen-specific VIL.**  
726 **a,** Representative flow-cytometric analysis showing expression of CD45RO, CD45RA and CD62L among  
727 enriched and expanded CMV-specific CD8<sup>+</sup> T cells at day-7. **b,** Summary of Naïve, Central memory and  
728 effector memory T cells subsets from data obtained in a, (*n*=4). **c,** Analysis as in a, for SARS-CoV-2-  
729 specific CD8<sup>+</sup> T cells, and **d,** analysis as in b, for SARS-CoV-2-specific CD8<sup>+</sup> T cells (*n*=8).

730

731 **Fig. 5: Proinflammatory cytokine expression among rapidly-expanded SARS-CoV-2 and CMV**  
732 **antigen-specific VIL. a,** Representative flow-cytometric analysis showing expression of IFN- $\gamma$  and TNF $\alpha$   
733 among enriched and expanded SARS-COV-2 CD8<sup>+</sup> T cells at day-7, after 6-hour stimulation with specific  
734 peptide antigen, and proportions of IFN- $\gamma$ /TNF $\alpha$  expressing cells also expressing IL-2. **b,** Summary of



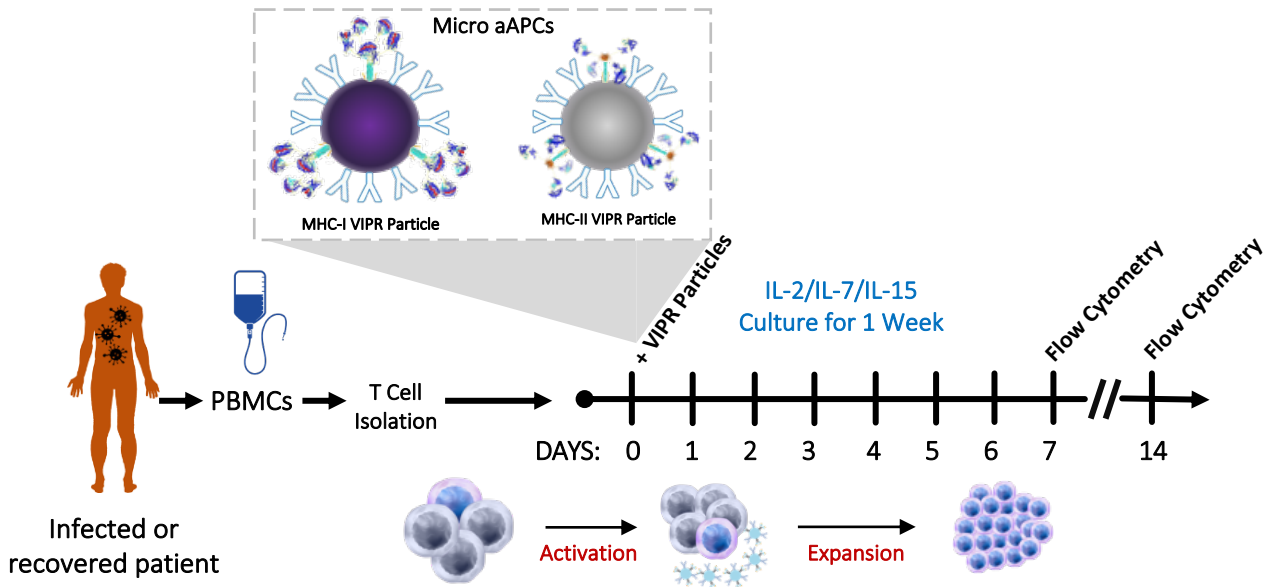
735 the data obtained as in a for each cytokine ( $n=7$ ). **c**, Representative proportion of SARS-CoV-2 CD8<sup>+</sup> T  
736 cells expressing 1, 2 or 3 cytokines. **d**, Extended analysis of SARS-CoV-2 VIL polycytokine function as  
737 SPICE representation. **e**, Analysis as in a, for CMV-specific CD8<sup>+</sup> T cells. **f**, Histograms analyzed as in b  
738 summarizing the data obtained with CMV antigen specific CD8<sup>+</sup> T cells ( $n=3$ ). **g**, Representative  
739 proportion of CMV CD8<sup>+</sup> T cells expressing 1, 2 or 3 cytokines. **h**, Extended analysis of CMV-specific VIL  
740 polycytokine function as SPICE representation.

741

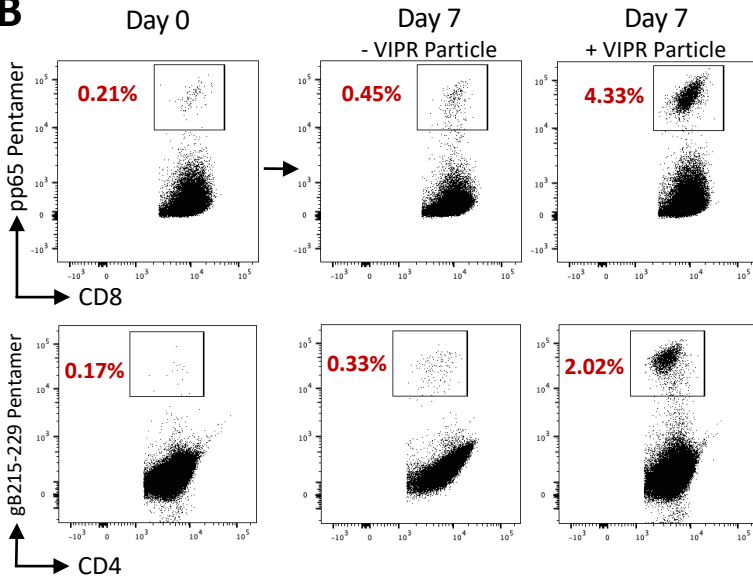
742 **Fig. 6: Allogeneic VIL Therapy Platform: An adoptive cell therapy for the treatment of individuals**  
743 **suffering from severe symptoms of COVID-19.** **a**, Schematic for a COVID-19 cell therapy in which  
744 PMBCs are collected from the blood of HLA-typed hospitalized patients and total T cells isolated. T  
745 cells are stimulated with HLA-matched MHC-I/MHC-II antigen-specific SARS-CoV-2 VIPR beads to  
746 enrich and expand CD4<sup>+</sup> and CD8<sup>+</sup> T cells with TCRs specific for the SARS-CoV-2 antigen epitopes. These  
747 antigen-specific VIL expand at an average of 1,000-fold prior to adoptive transfer back to HLA-matched  
748 patients to mediate a T cell immune response to support the eradication of the SARS-CoV-2 virus and  
749 to engender protective immunity against repeat infection. **b**, Estimations of viral-specific T cell  
750 numbers generated ex vivo for patient infusion based on the empirical data of VIL expansion by VIPR  
751 particles.

# Figure 1

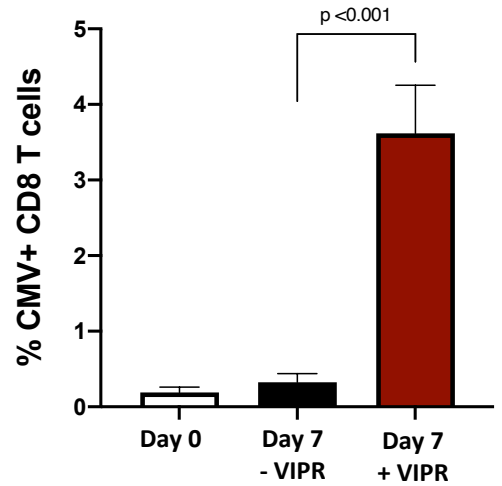
## A



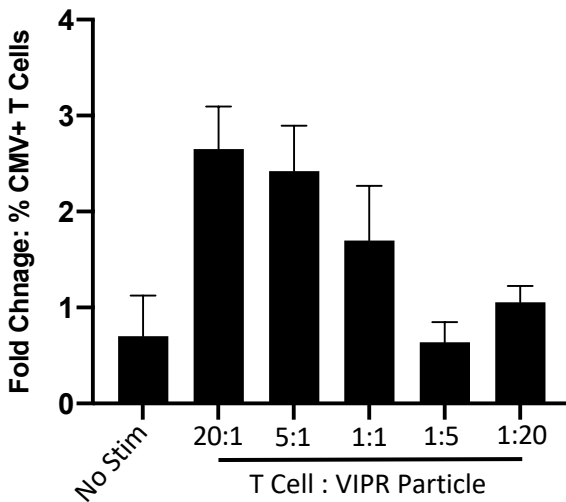
## B



## C



## D



## E

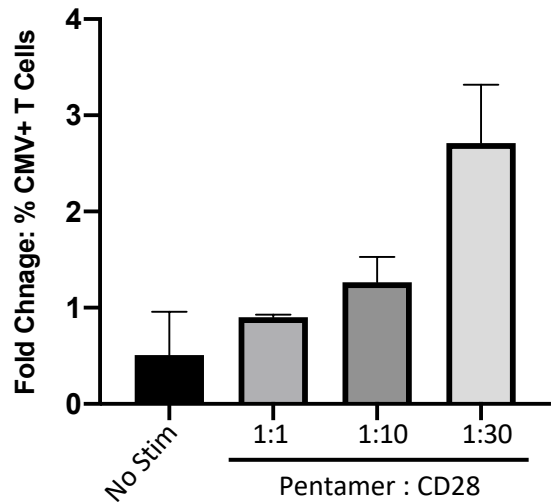
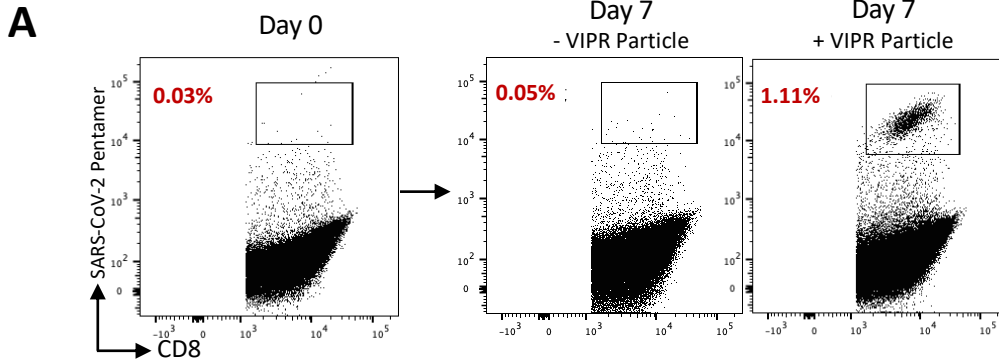


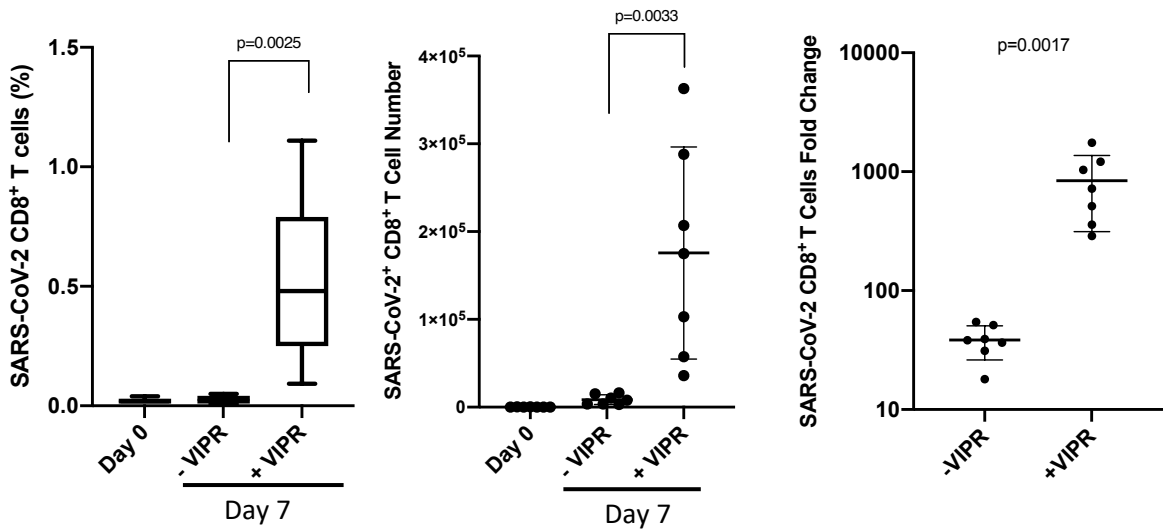
**Figure 2**



**B**

Donor	Sex	Age	Serological Results	Days post infection PBMCs harvested	Symptoms	MCH-I	% VIL (day 0)	Fold change by VIPR expansion
1	F	37	IgG+ / IgM+	25	Fatigue; Non-productive cough; Shortness of breath; Anosmia	HLA-A2 02:01	0.03	37
2	M	48	IgG+ / IgM+	72	Fever >100.4°F; Chills; Muscle aches; Headache; Ageusia & Anosmia	HLA-A2 02:01	0.02	21
3	M	46	IgG+	53	Sore throat; Nasal congestion; Fatigue; Non-productive cough	HLA-A2 02:01	0.02	10
4	M	42	IgG+	26	Fever >100.4°F (38C), Congestion; Non-productive cough; Chills; Flu-like symptoms; Muscle aches; Fatigue;	HLA-A2 02:01	0.01	48
5	F	42	IgG+ / IgM+	24	Headache; Fever >100.4°F; Muscle aches; Ageusia & Anosmia; arthralgias; Fatigue; Non-productive cough	HLA-A2 02:01	0.02	16
6	M	51	ND	28	ND	HLA-A2 02:01	0.04	19
7	M	49	ND	26	ND	HLA-A2 02:01	0.01	12

**C**



**D**

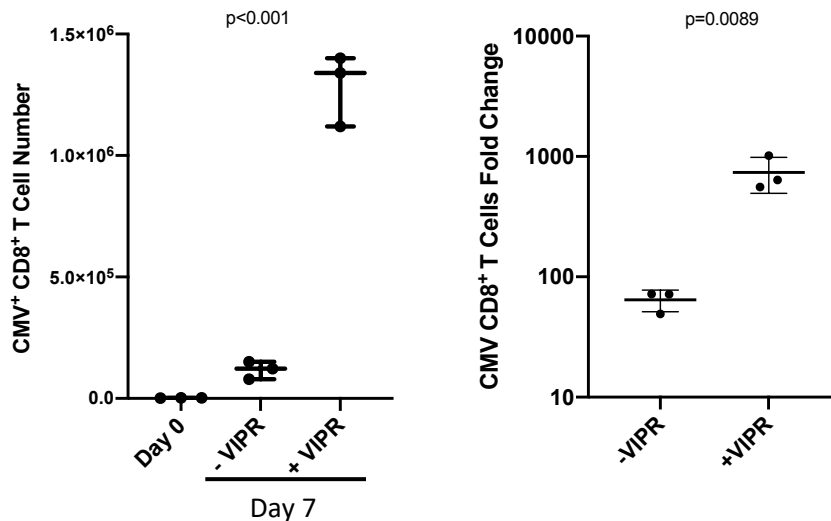
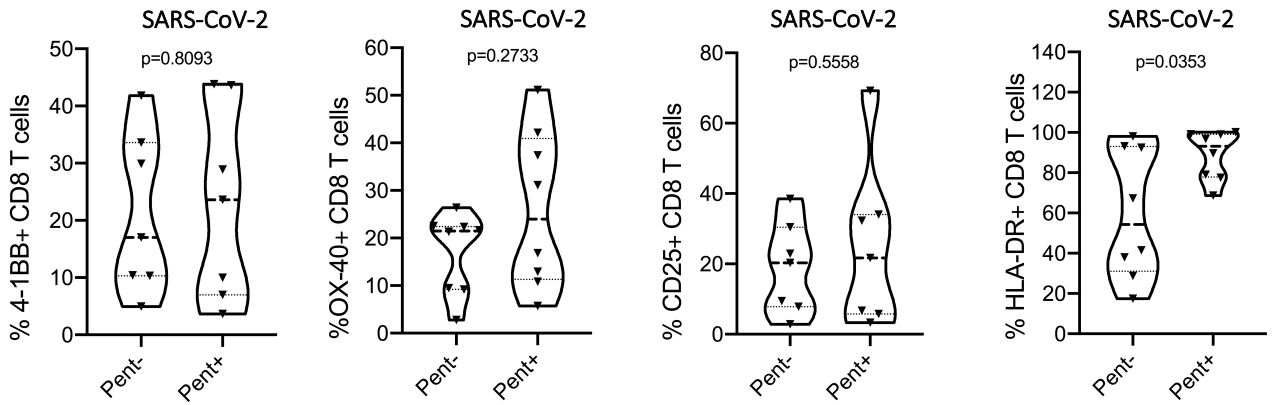
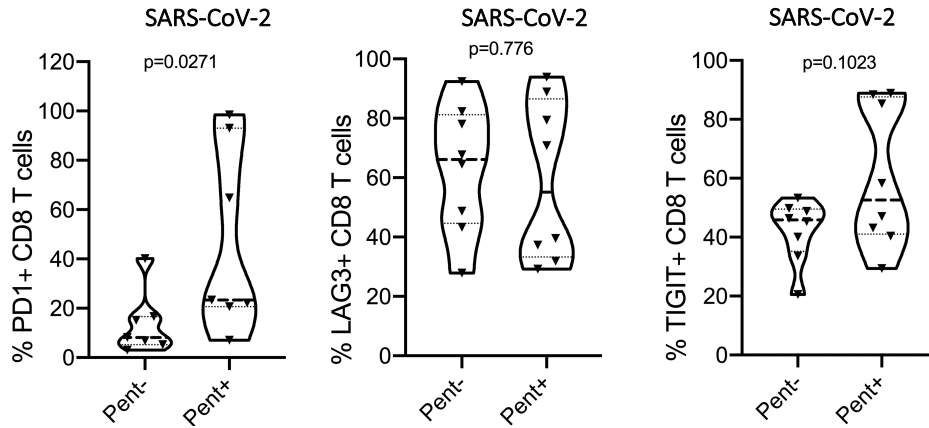


**Figure 3**

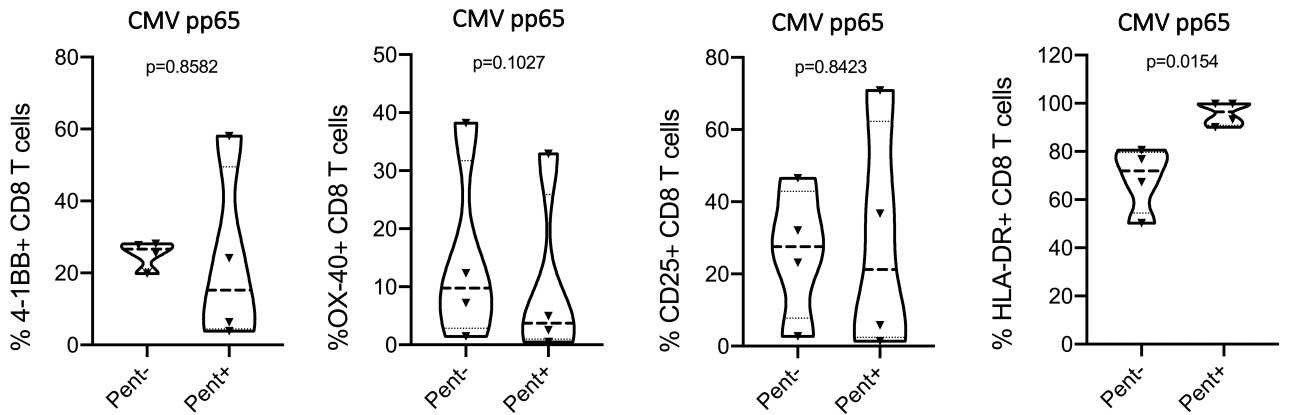
**A**



**B**



**C**



**D**

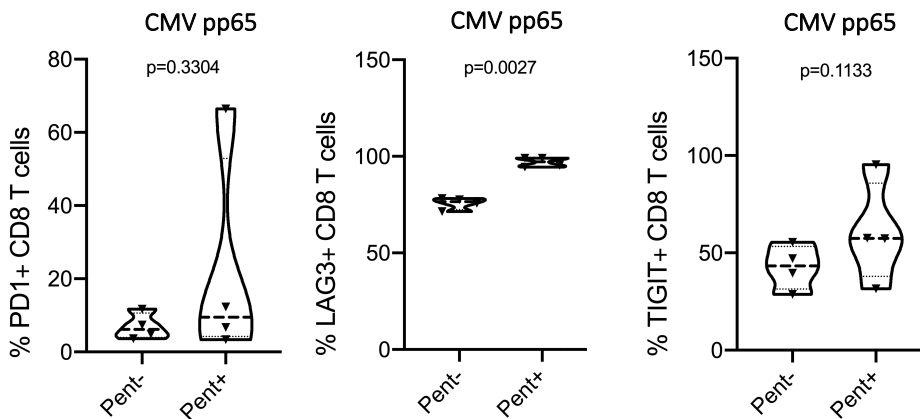


**Figure 4**

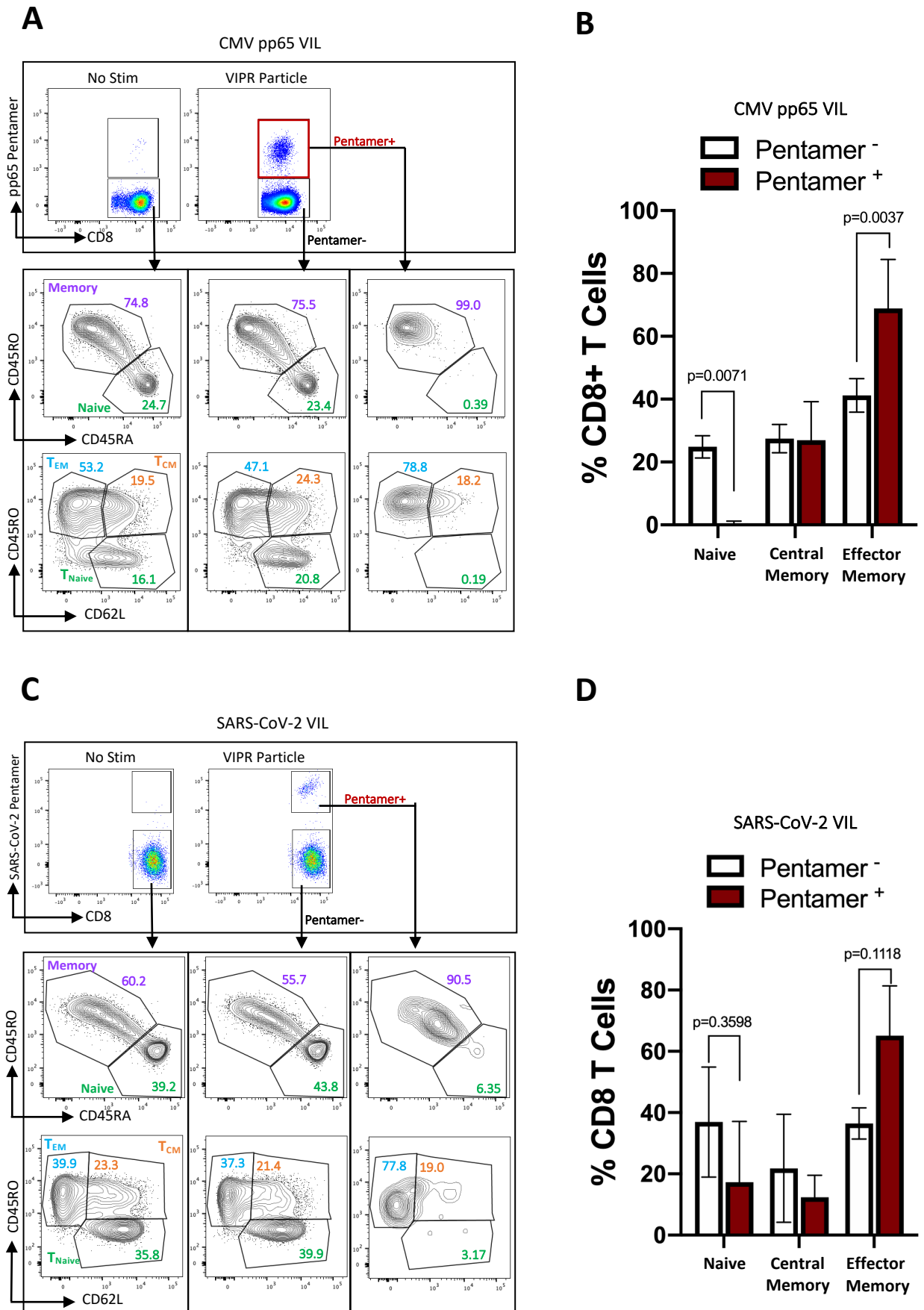
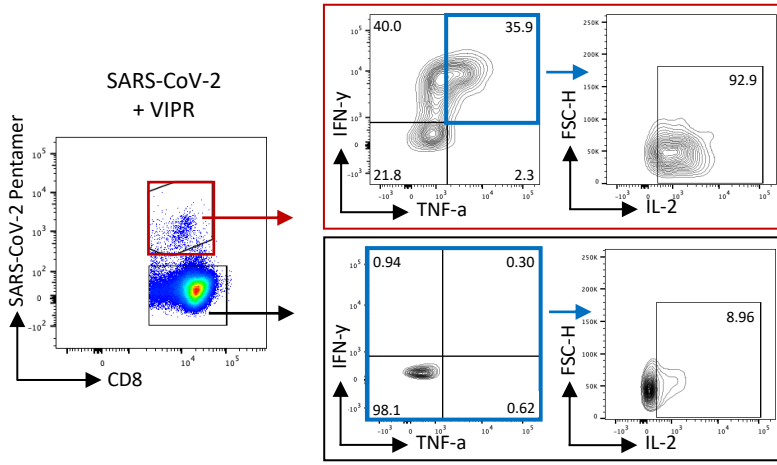
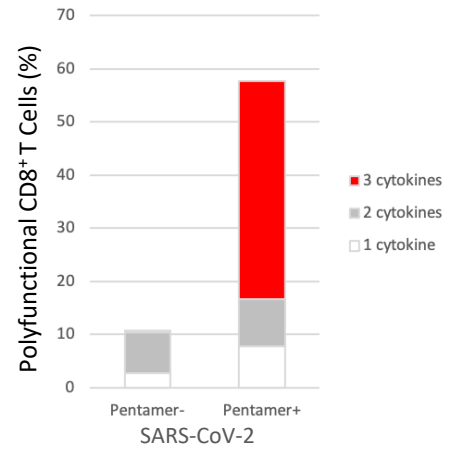


**Figure 5**

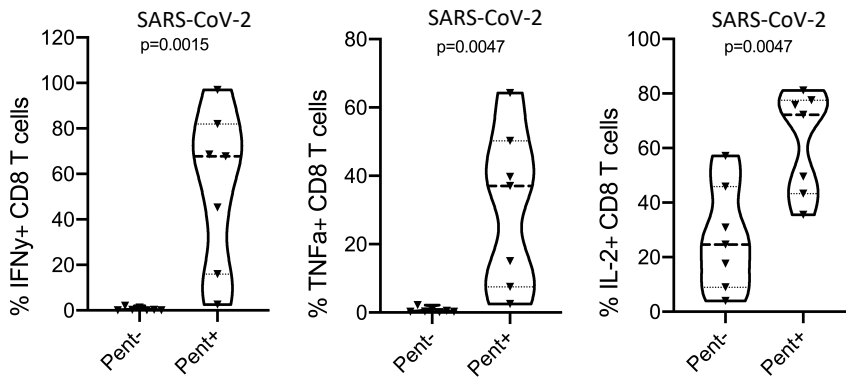
**A**



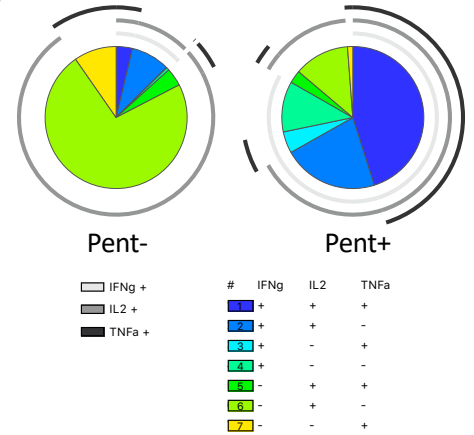
**C**



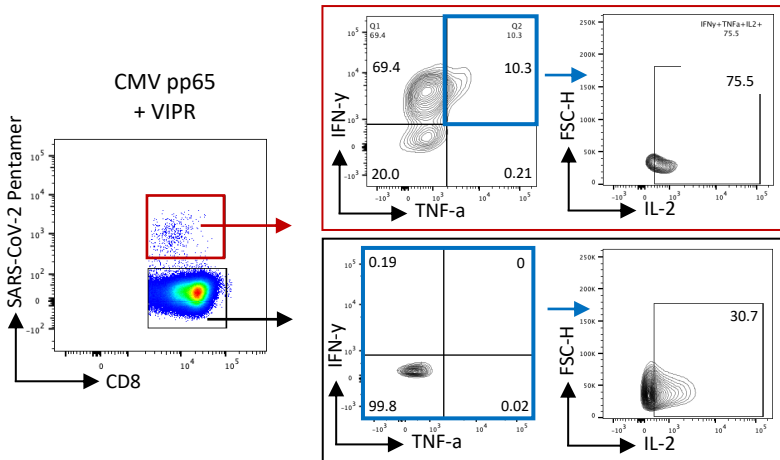
**B**



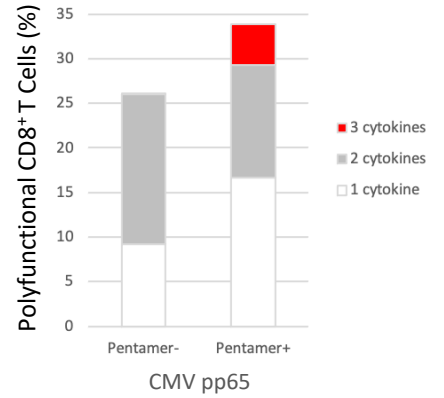
**D**



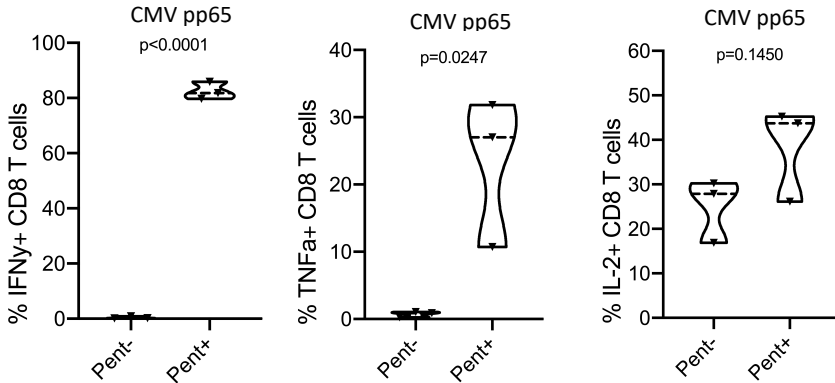
**E**



**G**



**F**



**H**

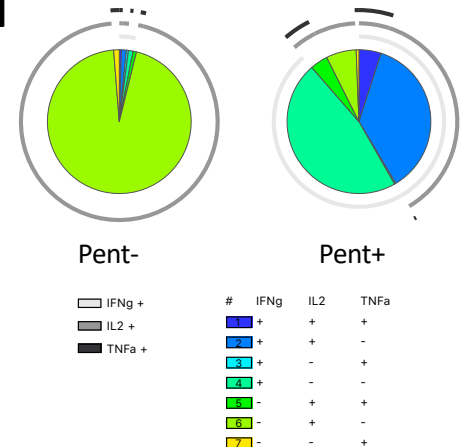
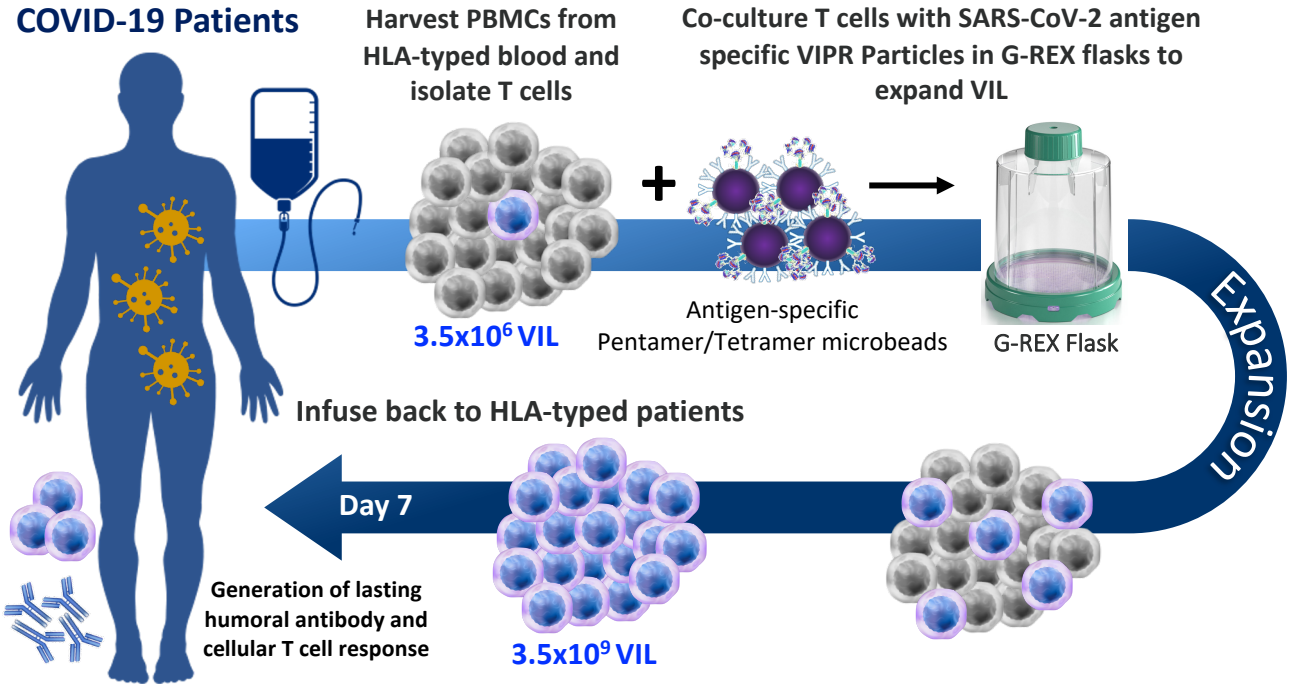


**Figure 6**

**A**



**B**

Therapeutic Parameters	Value
Volume of blood per kg of bodyweight that can be taken from a patient	5 ml / kg
Therefore, approx. total volume of blood for T cell extraction in 70kg male	350 ml
Number of total T cells per ml of blood	1x10 <sup>6</sup>
Total number of T cells extracted per patient	3.5x10 <sup>8</sup>
Estimated % of SARS-CoV-2 VIL during infection	1%
Total number of SARS-CoV-2 VIL isolated per patient	3.5x10 <sup>6</sup>
Average fold-expansion of SARS-CoV-2 VIL ex vivo after 7 days	1,000-fold
<b>Total number of expanded SARS-CoV-2 VIL for patient infusions</b>	<b>3.5x10<sup>9</sup></b>